ELSEVIER

Journal of Alloys and Compounds 434–435 (2007) 459–462

Journal of ALLOYS AND COMPOUNDS

www.elsevier.com/locate/jallcom

Deformation-induced alloying and reactions in nanostructured multilayers

J.H. Perepezko [a,*], R.J. Hebert [b], J. Hamann [c]

[a] *University of Wisconsin-Madison, Department of Materials Science and Engineering, 1509 University Avenue, Madison, WI 53706, USA*
[b] *Chemical, Materials and Biomolecular Department of Engineering, University of Connecticut, Storrs, 97 N Eagleville Rd., Storrs, CT 06269, Germany*
[c] *Xtalic Corporation, 200 Boston Ave., Suite 4100, Medford, MA 02155, USA*

Available online 13 October 2006

Abstract

Deformation-induced alloying reactions in multilayers depend on the refinement of the layer structure and the atomic-scale mixing at the interfaces. Under intense deformation of multilayer samples, a nanometer-scale layer thickness and grain size develops during repeated cold rolling. As the length scale of the layer thickness converges to that of the interfacial mixing zone during rolling, alloying and amorphization can develop in appreciable volumes. The relative specific interfacial area is then a key metric to describe deformation-driven alloying. The examination of amorphous Al alloys suggests that the deformation-induced crystallization reactions could be linked to quenched-in atomic arrangements that are also evident from structural studies. Deformation-induced devitrification reactions depend on the formation of shear bands and therefore implicitly on the process conditions.

Keywords: Amorphous material; Nanostructures; Mechanical alloying; Scanning and transmission electron microscopy; Thermal analysis

1. Introduction

One of the highlights of the contemporary attention directed towards nanocrystalline materials is the major innovation in processing methodologies that have been developed to achieve nanostructured materials. These efforts have yielded a large variety of methods based upon strategies involving vapor, liquid and solid state processing [1] that can be considered in two broad categories based upon the manner in which the driving free energy that motivates structural changes is developed during processing.

A useful concept for the study of non-equilibrium processes is the distinction between closed and open system processes. In a closed system, an energized state is achieved through an initial rapid temperature, pressure or composition change to create a certain level of undercooling or supersaturation (i.e. a metastable state), which then relaxes towards equilibrium by diffusion during annealing. With an open system, the energized state is often attained by a continuous incremental input to an initial state through the incorporation of excess lattice defects or solute on a localized spatial scale and time interval that is short compared to the relaxation time [2]. During processing, some relaxation is possible and can be expressed by a saturation of stored energy (i.e. minimum grain size) [3]. Moreover, the key feature of open systems is the modification of the kinetic pathways by the continued dynamic input [4,5]. These systems are also identified as driven systems in the sense that the kinetics are driven by the external input to new pathways and new microstructures. While the deformation of multilayer samples has been studied mainly within the context of mechanics of composites, intense deformation can lead to structural transformations that include amorphization reactions of multilayer samples [4–9].

The difference in the phase evolution between a closed system process such as rapid solidification, RSP and driven system processing can be considered further based on the schematic phase diagram depicted in Fig. 1. The RSP route is denoted with the vertical line that is close to the eutectic composition. The isothermal cold-roll process is represented by the horizontal line. For both processing routes the positions of the T_0 lines are important. The T_0 lines mark the stability limit for a crystalline phase [10]. Any closed system technique that aims at the synthesis of amorphous phases therefore should treat an alloy with a composition between the T_0 curves at temperatures below the glass transition temperature. Although the schematic phase diagram in Fig. 1 is

* Corresponding author. Tel.: +1 608 263 1678; fax: +1 608 262 8353.
E-mail address: perepezk@engr.wisc.edu (J.H. Perepezko).

0925-8388/$ – see front matter © 2006 Elsevier B.V. All rights reserved.
doi:10.1016/j.jallcom.2006.08.105

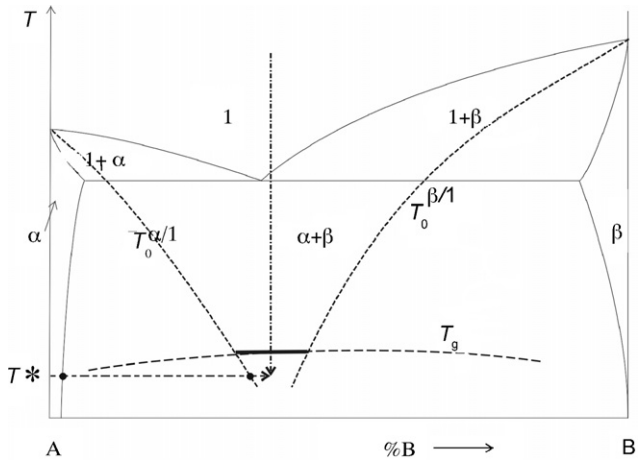

Fig. 1. Schematic binary eutectic phase diagram including T_0 and T_g curves.

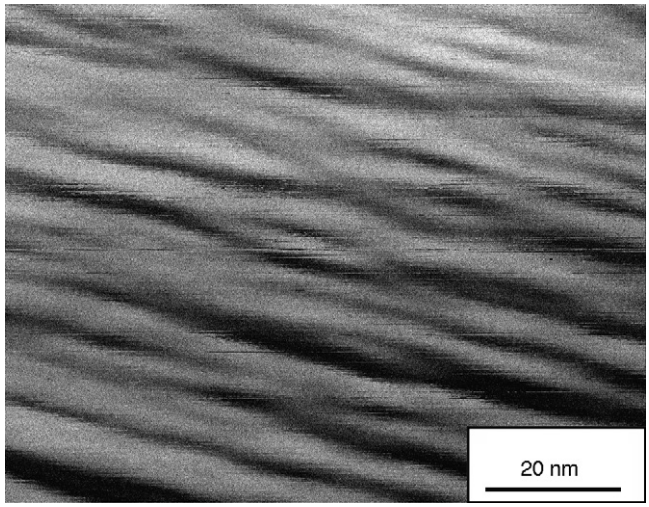

Fig. 2. Cross-sectional STEM dark-field image of the $Al_{66}Pt_{34}$ multilayer at a strain of −38.

useful for the thermodynamic aspects of the phase evolution, it does not reflect the influence of the heterogeneous structure on the alloying process of the multilayers. During the isothermal deformation process of multilayers, by contrast, concentration differences exist in the sample that result from localized mixing reactions at the interfaces. It is therefore important to keep in mind that the horizontal pathway depicted in Fig. 1 reflects local composition changes while the nominal composition of the multilayer remains constant.

The understanding of the role of alloying in promoting glass formation is under active study [11], but the guidelines for component selection are established [12]. Along with the advances in basic understanding there has been a recognition that the structural models of amorphous alloys require refinements to account for local interactions that represent short range order as well as the development of medium range order [11,13–15]. These are important issues that impact the analysis of the crystallization behavior, thermal stability and deformation behavior where there is clear evidence that deformation can induce crystallization without thermal annealing [16–19]. In the current discussion some highlights of the reactions in Al-based multilayers involving both melt spun amorphous ribbon and crystalline layers during repeated rolling and folding are examined to expose the controlling parameters and to develop a mechanistic understanding.

2. Deformation-induced alloying

A precondition for deformation-induced phase transformations is a mixing reaction at interphase boundaries. In multilayer samples there is now clear evidence from experiments and simulation that the mixing reactions occur on a nanostructured size scale and yield a true alloying analogous to interdiffusion. However, the nanoscale processes controlling the mixing are more complex that single atom jumps.

The foils used for the rolling experiments have an initial thickness of micrometers, so that the nanoscale thickness of the mixing layer that follows an atomic scale process is small compared with the layer thickness during the initial deformation stage. The repeated folding and rolling process of the multilayers that was conducted with a hand rolling mill in air at room temperature and at a strain-rate of approximately 0.1 s^{-1} leads to a gradually increasing fraction of atoms in the mixing volume at the interfaces. For systems that can undergo extensive refinement of the layer structure such as the Al–Pt multilayer that is depicted in cross-section in Fig. 2 (initial layer thickness: 25 μm) at a strain of −38, the fraction of atoms that are in the mixing or alloying volume is therefore significant.

For an $Al_{66}Pt_{34}$ multilayer, complete amorphization has been obtained by repeated rolling at liquid nitrogen temperature [20]. The rolling experiments at room-temperature indicated that the Al peaks disappeared while a broad amorphous peak formed simultaneously in the X-ray pattern [20]. The calculation of the T_0 limits at room-temperature indicates that in the composition range between 22 at.% Pt and 43 at.% Pt the fcc phase is unstable with respect to the undercooled liquid (i.e. amorphous) phase [21]. Based on the T_0 boundaries and the STEM concentration measurements, the complete amorphization reaction in the Al–Pt multilayer occurs in two steps, the driven dissolution of the fcc-Al phase in the first step and the slower mixing between the amorphous phase and the fcc-Pt in the second step. Since the fcc-Al phase dissolves while an amorphous phase develops, the mixing that occurs initially at the interface between the Al and Pt layers must take place between fcc-Al and the amorphous phase until the fcc-Al phase has dissolved. Complete amorphization then requires mixing between the amorphous phase and the remaining fcc-Pt phase that becomes increasingly important at high deformation levels. This is consistent with the large driving free energy that motivates initial mixing and is reduced following the initial formation of an amorphous layer [22].

3. Structural diagnostics

A characteristic of driven system behavior is a sensitivity of the structural evolution during processing to the initial state. In amorphous Al alloys the primary crystallization develops from

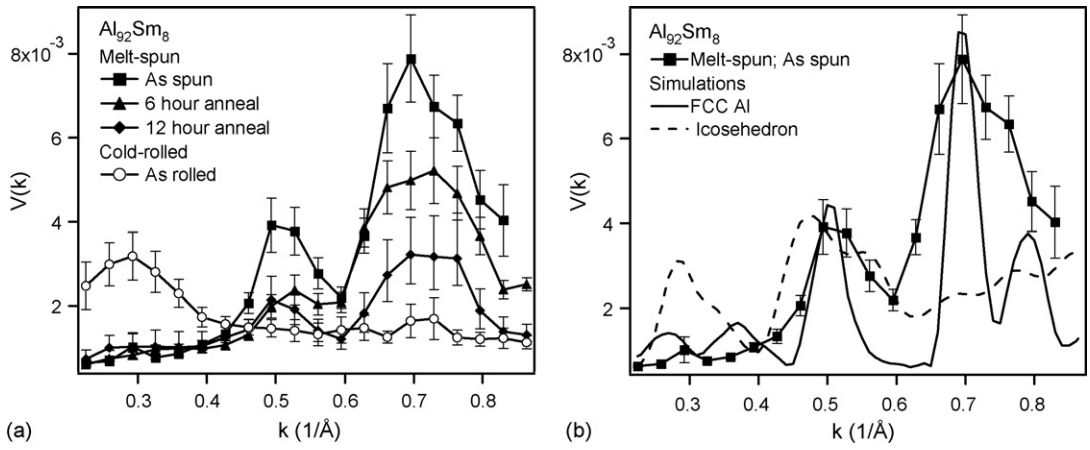

Fig. 3. (a) Fluctuation microscopy data $V(k)$ for melt-spun as spun, 6 h, and 12 h annealed, and cold-rolled $Al_{92}Sm_8$. (b) Measured $V(k)$ for melt-spun as spun and simulated $V(k)$ for a 30 Å Al sphere and a Sm-centered icosahedron. The Al sphere reproduces the peak positions and relative heights.

heterogeneities that are retained during the quenching of the alloy from the liquid state. The liquid alloys rapidly solidify while being ejected onto a Cu-wheel that rotates with a surface tangential speed of about 55 m/s in an inertgas atmosphere. Some further insight into the nature and effect of the heterogeneities has been developed through studies of medium range order, MRO and the influence of selected alloying.

Fluctuation electron microscopy, FEM measures diffraction from nanoscale volumes using dark-field transmission electron microscopy (TEM) at a deliberately low (5–50 Å) image resolution [15]. The magnitude of the spatial fluctuations in diffraction, measured by the normalized variance V as a function of scattering vector k, gives information about MRO at the length scale of the image resolution. The MSR $V(k)$ shown in Fig. 3a for the $Al_{92}Sm_8$ sample arises from nanoscale Al-like order. The peaks at 0.5 and 0.7 $Å^{-1}$ correspond to the Al ⟨2 0 0⟩ and ⟨2 2 0⟩ reflections. The second peak also covers the Al ⟨3 1 1⟩ at 0.82 $Å^{-1}$. Fig. 3b shows $V(k)$ simulated for both a 30 Å diameter crystalline Al sphere and icosahedron of 12 Al atoms surrounding a Sm atom. The Al model reproduces both the peak positions and the relative peak heights in the MSR $V(k)$. Icosahedron and $Al_{11}Sm_3$ and Al_4Sm sphere simulations (not shown) fail to reproduce even the experimental peak positions. What is required is diffraction from some Al Bragg condition that is spatially heterogeneous on a length scale of 16 Å, the spatial resolution of the imaging. This means atoms locally organized into an fcc Al lattice (possibly strained or distorted); thus, nanoscale Al-like order. The MRO measurements support the model that primary crystallization in these alloys is driven by Al clusters formed during the quench, then frozen into the structure [23]. At a given annealing temperature, some of those clusters are supercritical and grow into stable crystals, which accounts for the observed decrease in nucleation rate under isothermal annealing. Fig. 3 shows that the degree of MRO, indicated by the height of the peaks, is reduced by the isothermal anneal. However, a large crystal in the field of view will dominate the $V(k)$ signal from the surrounding material, so that these are avoided in the FEM measurements. That means that in the annealed samples, the remaining population of clusters is measured; not the crystallized material. Moreover, based on the final nanocrystal density, it is estimated that there are on order of 10 supercritical clusters per 0.3 μm × 0.3 μm micrograph.

It is known that small additions of Cu to several Al-based glass forming compositions effectively refine the grain size of the primary phase nanocrystals [23]. Unlike similar Cu additions to Fe-based amorphous alloys, the Cu atoms have not been shown to cluster in the amorphous Al matrix. Substitutions for Ni ranging from 0.05 to 2.0 at.% were made to $Al_{88}Ni_8Sm_4$ to investigate whether increasing levels of Cu substitution causes a gradual decrease in the mean nanocrystal size, or whether there exists a threshold Cu level to affect the size and distribution of primary phase nanocrystals.

Results from continuous heating DSC measurements in Fig. 4 show that the onset of the primary crystallization onset temperature is measurably depressed in a continuous manner to a lower temperature with Cu substitution levels as low as 0.2 at.%.

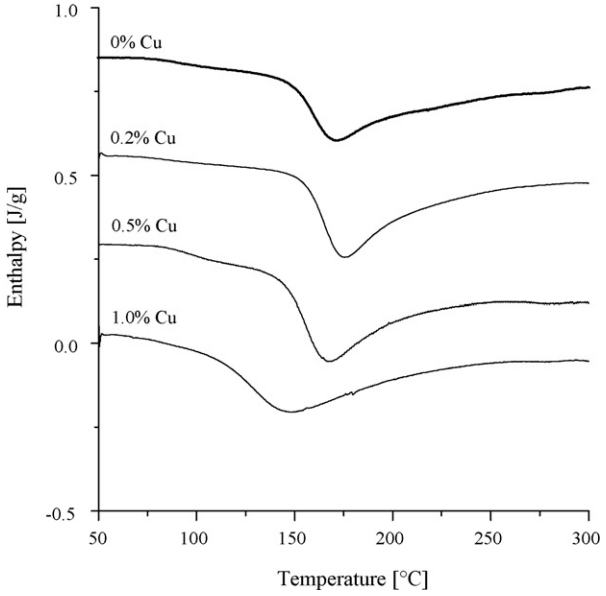

Fig. 4. DSC traces of $Al_{88}Ni_{8-x}Sm_4Cu_x$ alloy; $dT/dt = 20$ K/min.

From an analysis of TEM measurements, the average nanocrystal diameter is refined from 9.7 to 7.5 nm with substitution of 1 at.% Cu for samples annealed at 140 °C for 10 h. This behavior suggests that the influence of Cu substitutions is continuous and provides an enhanced site density for nanocrystal development.

4. Deformation-induced transitions

A main concept in the theory of driven system processing is the competition between partial processes that tend to move the system closer to equilibrium or more towards a non-equilibrium state [24]. The observation of cold-rolling induced amorphization of crystalline multilayers during intermixing is one clear example of a transition towards non-equilibrium. On the other hand, deformation-induced crystallization [16–19] is an example of a transition towards equilibrium. However, if both types of transitions are possible, the effect of the cold-rolling process on the amorphous phase may be the creation and disintegration of nanocrystals, resulting in a dynamic steady-state for the nanocrystallite size and density [25]. Indeed, a cyclic crystalline-to amorphous transformation might occur during the deformation processing, similar to the cyclic transformation behavior of ball-milled Co–Ti and Al–Zr powders [26]. This demonstrates that the driven system technique offers opportunities for microstructure control that cannot be achieved by thermal processing.

Deformation-induced crystallization reactions have been identified for several Al-based amorphous alloys, for example the Al88Y7Fe5 alloy, the Al90Fe5Gd5 alloy, or other alloys that are summarized in [27]. Some Al-based amorphous alloys, however, remain amorphous during intense deformation, for example the Al85Ni10Ce5 alloy. Alloys that reveal deformation-induced crystallization also reveal primary crystallization during continuous heating while the alloys such as the Al85Ni10Ce5 alloy that remain amorphous reveal a more complex crystallization behavior. Since the results of the FEM analysis suggest that the primary crystallization develops from quenched-in structural heterogeneities, it seems conceivable that the structural heterogeneities could play a key role for the deformation-induced crystallization reactions [27,28].

5. Summary

The systematic investigation of the cold rolling of elemental multilayer samples has demonstrated the versatility of this technique in important new areas. The rolling can induce an amorphization in crystalline multilayers of strong glass formers as well as Al-based marginal glass formers without any annealing. An essential outcome of the several rolling experiments is that the common glass-forming ability criteria used for liquid quenching cannot rigorously be applied to cold rolling. Instead, evidence has been found that criteria for rolling induced amorphization have to be related to mechanical properties (ductile behavior, crystal structure, melting temperature) as well. The FEM investigation of Al–Sm has led to the very important result that the rolling-induced amorphous phase is structurally different from the melt-spun amorphous phase with the same composition. Quenched-in nuclei have been identified as the reason for this difference. The experiments furthermore demonstrated that the rolling-crystallization is not caused by temperature effects in the sample during rolling. The current understanding rather points towards a mechanical process inducing crystallites. These are new developments that offer exciting possibilities for control of nanoscale microstructures and also represent new challenges for the fundamental understanding of the reaction mechanisms involved in synthesis and processing.

Acknowledgement

The support of the ARO (DAAD 19-02-1-0245) is gratefully appreciated.

References

[1] H. Gleiter, Progr. Mater. Sci. 33 (1989) 223.
[2] G. Martin, Phys. Rev. B 30 (3) (1984) 1424.
[3] W.L. Johnson, Progr. Mater. Sci. 30 (1986) 81.
[4] G. Martin, P. Bellon, Solid State Phys. 50 (1997) 189.
[5] R.A. Enrique, P. Bellon, Phys. Rev. Lett. 84 (13) (2000) 2885.
[6] R.J. Hebert, J.H. Perepezko, Scr. Mater. 49 (2003) 933.
[7] R.J. Hebert, J.H. Perepezko, Scr. Mater. 50 (2004) 807.
[8] F. Bordeaux, A.R. Yavari, P.J. Desré, Mater. Sci. Eng. 97 (1988) 129.
[9] R.J. Hebert, J.H. Perepezko, Mater. Sci. Forum 386–388 (2002) 21.
[10] J.H. Perepezko, W.J. Boettinger, in: L.H. Bennett, T.B. Massalski, B.C. Giessen (Eds.), MRS Proceeding, vol. 19, 1983, p. 223.
[11] T. Egami, J. Non-Cryst. Solids 317 (2003) 30.
[12] A. Takeuchi, A. Inoue, Mater. Trans. 43 (2002) 2275.
[13] T. Egami, Mater. Trans. 43 (2002) 510.
[14] E. Matsubara, S. Sato, M. Imafuku, T. Nakamura, K. Koshiba, A. Inoue, Y. Waseda, Mater. Sci. Eng. A 312 (2001) 136.
[15] W.G. Stratton, J. Hamann, J.H. Perepezko, P.M. Voyles, X. Mao, S.V. Khare, Appl. Phys. Lett. 86 (2005) 141910.
[16] R. Schulz, M.L. Trudeau, D. Dussault, A. Van Neste, J. Phys. 51 (C4) (1990) 259.
[17] H. Chen, Y. He, G.J. Shiflet, S.J. Poon, Nature 367 (1994) 541.
[18] R.J. Hebert, J.H. Perepezko, Mater. Sci. Eng. A 375–377 (2004) 728.
[19] W.H. Jiang, M. Atzmon, Acta Mater. 51 (2003) 4095.
[20] F. Bordeaux, A.R. Yavari, J. Appl. Phys. 67 (5) (1989) 2385.
[21] J.H. Perepezko, R.J. Hebert, Z. Metallkd. 94 (2003) 10.
[22] J.H. Perepezko, Composite Interf. 1 (1993) 463.
[23] J.H. Perepezko, R.J. Hebert, W.S. Tong, J. Hamann, H.R. Rösner, G. Wilde, Mater. Trans. JIM 44 (2003) 1982.
[24] P. Bellon, R.S. Averback, Phys. Rev. Lett. 74 (10) (1995) 1819.
[25] R.J. Hebert, J.H. Perepezko, H. Rösner, G. Wilde, Scr. Mater. 54 (2006) 25.
[26] M. Sherif El-Eskandarany, Mechanical Alloying, William Andrew Publishing, Norwich, 2001, p. 209.
[27] M. Gao, R.E. Hackenberg, G.J. Shiflet, Mater. Trans. JIM 42 (2001) 1741.
[28] R.J. Hebert, J.H. Perepezko, in preparation.